A photochemical model for the space-time variations of the oxygen allotropes in the 20 to 100 km layer

By JAMES R. BLANKENSHIP, *United States Air Force*[1]
and PAUL J. CRUTZEN, *International Meteorological Institute, Stockholm*[2]

(Manuscript received June 21, 1965)

ABSTRACT

Various photochemical models based upon the infinite-day assumption were investigated. The effect of the deletion of certain of the photochemical reactions was ascertained. An infinite-day model was developed in which none of the photochemical reactions were deleted.

A time-dependent model was developed by an integration over the day. This model provided the distribution of the three oxygen allotropes as a function of height, latitude, time-of-day, and meteorological conditions at a given time of year.

The results obtained from the time-dependent model were then compared with those from the infinite-day model and the actual observed data. It was found that the departures between the observed data and the infinite-day model were in many cases greater than the differences between the observed data and the time-dependent model.

The seasonal phase lag was obtained by an integration over one year. This lag is then shown as a function of time of year and height at a given latitude.

Table of symbols

a_{31} Ratio of the rate of change of ozone to rate of change of atomic oxygen.

C_0 The total number of oxygen atoms per unit volume, No./cm^3, at a given level in the earth's atmosphere.

e_2 The quantum efficiency of dissociation for molecular oxygen.

e_3 The quantum efficiency of dissociation for ozone.

h Planck's Constant $= 6.610 \times 10^{27}$ erg sec.

I_0 The number of photons per unit area, time and wave number.

J_2 The rate coefficient for dissociation of molecular oxygen, sec^{-1}.

J_3 The rate coefficient for dissociation of ozone, sec^{-1}.

k_1 The rate coefficient for the three body collision process producing molecular oxygen, cm^6/sec.

k_2 The rate coefficient for the three body collision process producing ozone, cm^6/sec.

k_3 The rate coefficient for the two body collision process producing two oxygen molecules, cm^3/sec.

M Unspecified gas molecule involved in the three body collision process.

$M\phi$ *Air mass correction factor for different zenith angles (approximately the secant correction up to 60°).*

N_1 Notation for concentration of atomic oxygen, No./cm^3.

N_2 Notation for concentration of molecular oxygen, No./cm^3.

N_3 Notation for concentration of ozone, No./cm^3.

N_m Notation for concentration of third-bodies, No./cm^3.

O_1 Atomic oxygen.

O_2 Molecular oxygen.

O_3 Ozone.

t Time.

Δt Time step.

V_2 The number of oxygen molecules in the vertical above a unit area, No./cm^2.

V_3 The number of ozone molecules in the vertical above a unit area, No./cm^2.

V_c The vertically integrated volume during the time-of-year when the adjustment to changing radiation is by the collisional processes.

[1] The work presented in this paper was done during a stay at the International Meteorological Institute, Stockholm.

[2] Contribution No. 178.

V_R The vertically integrated volume during the time-of-year when the adjustment to changing radiation is by molecular dissociation.
$V\phi$ The optical depth $= V_2 \cdot M\phi$ or $V_3 \cdot M\phi$.
x Ratio of ozone concentration at any given time to its solar noon value.
α_2 Molecular absorption cross-section of molecular oxygen.
α_3 Molecular absorption cross-section of ozone.
ν The wave number of the radiation.
τ Time defined by $t \leqslant \tau \leqslant t + \Delta t$.
ϕ Zenith angle.

Introduction

The importance of ozone in the earth's atmosphere as a heating and cooling agent has been shown by PLASS (1956), OHRING (1958), LEOVY (1963) and others. Ozone is also an important agent in the study of atmospheric circulations. HESSTVEDT (1963) has shown that the three oxygen allotropes below 30 km and above 90 km have a relatively long life. The departures in the upper portion of the ozone profile, about 100 km, from the photochemical distribution have been shown by NICOLET (1960) to be a result of the time required for diffusion being shorter than the time required for photochemical recombination or dissociation at these levels.

The validity of most circulation studies involving ozone in some way depends on knowledge of what the distribution would have been in the absence of such processes as transport and diffusion. After CHAPMAN's (1930) discovery of the rapid dissociation of oxygen above 100 km, many model atmospheres have been developed which closely approximate the distribution of the three allotropes of oxygen. These models have been based on different rate coefficients and in some cases different forms of the photochemical equations. The aim of this paper is to develop a time-dependent model which will provide the height distribution of ozone as a function of location, time of year, time of day and meteorological conditions in the absence of transport and diffusion. In order to accomplish this aim it is necessary first to analyze the infinite-day approximations that have been used as to the effect of deleting certain of the photochemical reactions, the degree of sensitivity of the infinite-day distributions to various rate coefficients, and the effect of various temperature distributions and zenith angles. The infinite-day models under consideration are those of HESSTVEDT (1963), LONDON (1962) and LEOVY (1963).

Two main assumptions are made throughout this study; first, that the time required for diffusion is long in comparison to the time required for photochemical dissociation or recombination in our height range of interest 20 to 100 km. Second, that the only reactions allowed occur between atomic oxygen, molecular oxygen and ozone.

The first of the above assumptions should not produce significant errors below about 100 km according to the findings of NICOLET (1960). However, the second assumption will produce errors in the distribution near 70 km. HESSTVEDT (1965) has shown that the introduction of hydrogen reactions in the photochemical equations tends to have little effect on molecular oxygen but appreciable effects on ozone in the 70 km region. However, this difficulty although serious does not directly affect the aim of the present study in that all models considered are based only on reactions between the three oxygen allotropes.

Photochemical reactions

The chief photochemical reactions involving the formation and distribution of ozone are assumed to be

$$O_2 + h\nu \rightarrow O_1 + O_1 \qquad J_2, \tag{1}$$

$$O_3 + h\nu \rightarrow O_1 + O_2 \qquad J_3, \tag{2}$$

$$O_1 + O_1 + M \rightarrow O_2 + M \qquad k_1, \tag{3}$$

$$O_1 + O_2 + M \rightarrow O_3 + M \qquad k_2, \tag{4}$$

$$O_1 + O_3 \rightarrow 2O_2 \qquad k_3. \tag{5}$$

The photochemical equations that express the above reactions may be written as:

$$dN_1/dt = 2J_2N_2 + J_3N_3 - 2k_1N_mN_1^2 - k_2N_mN_1N_2 - k_3N_1N_3, \tag{6}$$

$$dN_2/dt = k_1NmN_1^2 + 2k_3N_1N_3 + J_3N_3 - J_2N_2 - k_2N_mN_1N_2, \tag{7}$$

$$dN_3/dt = k_2N_mN_1N_2 - J_3N_3 - k_3N_1N_3. \tag{8}$$

The collisional rate coefficients k_1, k_2 and k_3 express the reaction rate for processes given in

equations (3), (4), and (5) respectively and are functions of the temperature to various degrees depending on whose model is used.

The photochemical rate coefficients J_2 and J_3 express the dissociation rates for the processes given in equations (1) and (2) respectively and may be expressed by

$$J_2 = \int_\nu e_{2_\nu} \cdot a_{2_\nu} \cdot I_{0_\nu} \cdot \exp - (a_{2_\nu} V_{2\Phi} + a_{3_\nu} V_{3\Phi}) \cdot d\nu, \tag{9}$$

$$J_3 = \int_\nu e_{3_\nu} \cdot a_{3_\nu} \cdot I_{0_\nu} \cdot \exp - (a_{2_\nu} V_{2\Phi} + a_{3_\nu} V_{3\Phi}) \cdot d\nu. \tag{10}$$

The data used to compute the dissociation rate coefficients were taken from LEOVY (1963). Leovy used the spectral energy distribution as arrived at by JOHNSON (1954). Below 2200 Å, Johnson found that the solar spectral irradiance curve is well approximated by the radiation which would be received from a blackbody source with the same size as the sun and having a temperature of 4500 degrees K.

Formulation of the infinte-day model

A form of a continuity equation can be arrived at from the complete mixing-condition: the total number of oxygen atoms in whatever state they exist must remain constant on a constant density surface. This constant is expressed by C_0 and the continuity equation becomes

$$N_1 + 2N_2 + 3N_3 = C_0 \tag{11}$$

which under the assumption of constant temperature profile is valid even at fixed heights.

If we now assume that the equilibrium state for the infinite-day model has been reached we may set $dN_1/dt = dN_2/dt = dN_3/dt = 0$ in equations (6), (7) and (8).

Multiply equation (7) by two and using the continuity equation to arrive at an expression for N_2 in terms of N_1 and N_3, i.e.

$$2N_2 = C_0 - N_1 - 3N_3,$$

equation (7) with the above operations becomes:

$$2k_1 N_m N_1^2 + 4k_3 N_1 N_3 + 2J_3 N_3 - J_2 (C_0 - N_1 - 3N_3) - k_2 N_m N_1 (C_0 - N_1 - 3N_3) = 0 \tag{12}$$

or rearranging the terms of equation (12) we obtain

$$N_3 (4k_3 N_1 + 2J_3 + 3J_2 + 3k_2 N_m N_1) + k_1 N_m N_1^2 - (J_2 + k_2 N_m N_1)(C_0 - N_1) = 0. \tag{13}$$

Solving for N_3 from equation (13) we find

$$N_3 = \frac{(J_2 + k_2 N_m N_1)(C_0 - N_1) - 2k_1 N_m N_1^2}{4k_3 N_1 + 2J_3 + 3J_2 + 3k_2 N_m N_1}. \tag{14}$$

Multiply equation (8) by two and using the continuity equation for $2N_2$ remembering that $dN_3/dt = 0$ gives:

$$k_2 N_m N_1 (C_0 - N_1 - 3N_3) - 2J_3 N_3 - 2k_3 N_1 N_3 = 0. \tag{15}$$

Solving for N_3 from equation (15) we find.

$$N_3 = \frac{k_2 N_m N_1 (C_0 - N_1)}{3k_2 N_m N_1 - 2J_3 + 2k_3 N_1}. \tag{16}$$

Setting equations (14) and (16) equal and factoring out N_1, we arrive at a third degree equation for N_1 in terms of k_1, k_2, k_3, J_2, J_3 and N_m which are all known for a given level.

$$N_1^3 (k_2 k_3 N_m - 3k_1 k_2 N_m^2 - 2k_1 k_3 N_m) + N_1^2 (-C_0 k_2 k_3 N_m - 4k_1 J_3 N_m - 2k_3 J_2) + N_1 (C_0 k_3 J_2 - J_2 J_3) + J_2 J_3 C_0 = 0. \tag{17}$$

This equation has one positive root, that is the infinite-day equilibrium value of atomic oxygen. Substituting the equilibrium value into equation (16) gives the equilibrium value of ozone. These two equilibrium values may be substituted into the continuity expression, equation (1), in order to obtain the equilibrium distribution of molecular oxygen.

Summary of results from infinite-day model

It was found that the difference between the various reduced photochemical equations (those in which certain reactions have been deleted) and the results obtained from the complete photochemical equations is not great except in the regions where the reduced equations change form. These differences are not quantitatively large but they do produce an effect on the slope of the ozone profile and, therefore, they may produce an effect on the cooling rate computed from these data. This effect would be

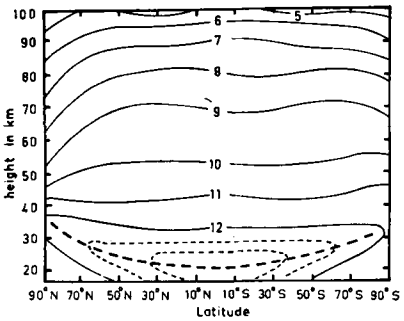

FIG. 1. Ozone concentration (number/cm³) in powers of 10 at the vernal equinox, summer temperatures profiles used in the southern hemisphere.

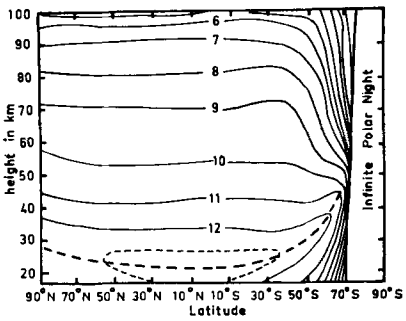

FIG. 2. Ozone concentration (number/cm³) in powers of 10 at the summer solstice, summer temperature profiles used in the nothern hemisphere.

brought about by either producing a too large or too small radiation flux divergence in these layers.

The analysis of the effect of various rate coefficients was more difficult. However, one striking difference was evident from the analysis of London's and Hesstvedt's rate coefficients. In London's case, the rate coefficients produce distributions that remain relatively unchanged with varying temperature distributions. In a meridianal cross section, such as is shown in Fig. 1 for the equinox, London's rate coefficients would produce a symmetric distribution about the equator even though different temperature distributions exist in the northern and southern hemispheres. As is shown by Fig. 1, Hesstvedt's rate coefficients produce a temperature dependent distribution and therefore a nonsymmetric distribution under varying temperature conditions. Such a distribution is in agreement with the observed seasonal variation at the 40 km level for Flagstaff, Arizona (Handbook of Geophysics, 1960). The 40 km level was selected for evaluation due to the minimum zenith angle effect occurring at that level. Fig. 2 shows the distribution for the summer solstice (northern hemisphere) and reflects both the temperature and solar angle dependence of the ozone distribution.

As a result of this analysis Hesstvedt's rate coefficients and the complete photochemical equation will be used as a first guess in the time dependent model.

The time-dependent model

The time-dependent equations (6), (7), and (8) must be used in order to obtain the distribution as a function of time-of-day (longitudinal variation). Such a time-dependent model must incorporate a varying solar radiation intensity as a function of the time-of-day. This model is then used to produce a photochemical distribution as a function of time-of-day, location and time-of-year and under known meteorological conditions.

The basic approach to the development of the time-dependent model may be summarized in the following steps:

1. The infinite-day solutions are modified and used as an initial guess.
2. The optical path for the radiation at a given latitude and time of the year but as function of the time of the day is arrived at through a consideration of the geometry of a curved atmosphere under the assumption of horizontal homogeneity.
3. A constant temperature profile is assumed in all cases.
4. Numerical integrations of equations (6), (7), and (8) in time with varying J_2 and J_3 are conducted until a convergence criterion is met.

Infinite-day initial guess for time-dependent model

By averaging over J_2 at 100 km during a 24 hour period an effective mean zenith angle was obtained for a given location and time of year. The validity of this method of selecting an average zenith angle will be discussed in the latter portion of this paper. This zenith angle was used in the infinite-day model to obtain the first guess of the mean concentrations of the

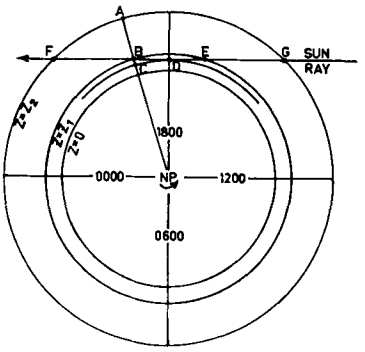

FIG. 3. Geometry of time dependent problem at the equator during the equinox, where $Z = 0$ represents the earth's surface, $Z = Z_1$ represents a height in the ozonosphere, $Z = Z_2$ represents the top of the earth's atmosphere.

oxygen allotropes, i.e. $N_1(Z)$, $N_2(Z)$ and $N_3(Z)$. The pressure at 20 km and the vertical temperature distribution is assumed to be independent of time-of-day but dependent on geographic location and time-of-year. With specified values of these meteorological parameters $N_m(Z)$, $k_1(Z)$, $k_2(Z)$, $k_3(Z)$, and $C_0(Z)$ were determined.

In order to proceed with an integration over a 24 hr period it was also necessary to compute the solar zenith angle (ϕ) as a function of time-of-day. It is then possible to compute the optical paths ($V\phi$) from the vertical concentrations of the absorbers at a given time and therefore the dissociation rate coefficients J_2 and J_3. These are assumed to be constant during a given time step and equations (6), (7), and (8) may be solved for the new concentrations of $N_1(Z)$, $N_2(Z)$ and $N_3(Z)$.

Computation of the optical path

We will consider the simplest case, that of the equinox condition at the equator. This is shown in Fig. 3. The radial coordinate represents the local solar time.

At solar noon (1200 hr) the dissociation rate coefficients (J_2 and J_3) may be computed without approximation since the integrated concentration from the top of the earth's atmosphere to level Z_1 exactly represents the optical path through which the radiation is passing. However, as one approaches 1800 hours the integrated concentration along the zenith times the zenith angle correction ($M\phi$) is less likely to represent the true optical path. In using this representation of the optical path one is essentially assuming a horizontally homogeneous distribution of the absorbers.

This method must be modified when the zenith angle exceeds 90°, that is, after 1800 hours and before sunset at 100 km and after sunrise at 100 km and before 0600 hours. From the geometry of the problem it is seen that the radiation reaching level Z_1 at B has passed through levels where the density of the atmosphere is greater than the density at the level Z_1. The optical path at point B may be expressed as the difference between twice the optical path at point D, which could represent the optical path through the total atmosphere along the line F, B, D, E, and G, and the optical path for point E, that is, along the line E to G. Under the assumption of horizontal homogeneity one may express the optical path to level Z_1 at point B, see Fig. 3, remembering that $V\phi = V(Z)\cdot M(\phi)$ by the following:

$$V\phi(B) = 2V(C)\cdot M(D) - V(B)\cdot M(E), \quad (18)$$

where

$V\phi(B)$ = optical path along the line B, D, E and G

$2V(C)M(D)$ = optical path along the line F, B, D, E and G

$V(B)M(E)$ = optical path along the line E to G

The vertical integrated volume is taken from the distribution along the radial A, B, C. The angle for the air mass correction factor ($M\phi$) is taken at the indicated points.

Alternatives to this assumption do exist. For example, if one could treat all latitudes at all times simultaneously it would in principle be possible to obtain the optical path in a more exact way. However, such a treatment requires large computer storage and furthermore requires some assumed distribution in order to calculate the optical path at sunrise. This is necessary since one is observing the sun through an optical path that has yet to be calculated. For these reasons the present model makes use of an assumption of horizontal homogeneity. This in effect slightly decreases the length of day at the ozone level.

Time steps and time constants

The time steps used in this model vary with the time of day (solar time); as long as the zenith angles are less than 75° a half hour time step is used. For the time period between a zenith angle of 75° and sunset or sunrise at 100 km, a 10 minute time step is used. The ten minute step is also continued for one hour after sunset and from one hour after sunset to sunrise a thirty minute step is used.

The reason for the use of the shorter time steps before sunset and just after sunrise is that these are the times of the greatest change in the optical depth for a given change in zenith angle. The shorter time period for the first hour after sunset is necessary in order to depict the rapid changes that occur during the first phase of night. That is, the rapid destruction of atomic oxygen and resulting buildup of ozone.

A simple forward time step method will lead to computational instability unless time steps on the order of one second or less are used. For the above reason a combined numerical and analytical method is developed for the time-dependent model.

Numerical solutions

An analysis of the terms contained in the photochemical equations and their variations in time and space has led to the definitions of 5 regions in each of which a specific numerical method for solution is used (see Fig. 4). The sizes of the regions change with latitude and time of year and some even disappear. In all the regions N_2, J_2 and J_3 are treated as constant during a time step for the calculation of new values of N_1 and N_3 at the end of the time-step but then also a new value for N_2 is determined by means of the continuity-equation (11). We now go over to a description of the five regions.

Region I

This is the region defined by the condition that $J_3 + k_3 N_1 > 0.8 \cdot 10^{-2}$. Here N_1 may be treated as being relatively constant during a time step and the solution of equation (8) at time τ, $t \leqslant \tau \leqslant t + \Delta t$ may be written:

$$N_3^\tau = N_3(E) + [N_3^t - N_3(E)] \exp[a(\tau - t)],$$

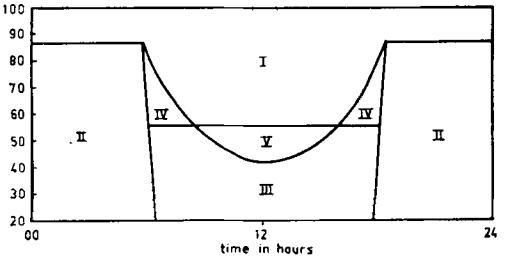

FIG. 4. Regions of solutions.

where $a = -J_3 - k_3 N_1^t$,

$b = k_2 N_m N_2 N_1^t$,

$N_3(E) = -b/a$ = the stationary solution of N_3 from eq. (8).

Under the defined condition for this region already when $\tau - t = 10$ minutes $\exp[a(\tau - t)] < 0.01$ and this together with the fact that a and b change very slowly assures us that we may set $N_3 = N_3(E)$ in this region at any time. The new value of N_1 at the end of the time step is now obtained by inserting $N_3 = N_3(E)$ in equation (6) and solving the resulting ordinary differential equation of the form

$$dN_1/dt = a N_1^2 + b N_1 + C,$$

with $a = -2k_1 N_m$,

$b = -k_3 N_3(E) - k_2 N_m N_2$,

$c = J_3 N_3(E) + 2 J_2 N_2$.

Region II

This is the region during night not included in region I. We make here the assumption that during a time step $t \leqslant \tau \leqslant t + \Delta t$

$$\left(\frac{dN_3/dt}{dN_1/dt}\right)^\tau = \left(\frac{dN_3/dt}{dN_1/dt}\right)^t = \frac{-(k_2 N_m N_2 - k_3 N_3^t)}{(k_2 N_m N_2 + k_3 N_3^t + 2k_1 N_m N_1^t)} = a_{31}.$$

At the beginning of night $a_{31} \approx -1$ because of the big size of $k_2 N_m N_2$ compared to $k_3 N_3$ and $k_1 N_m N_1$, but $k_3 N_3$ may later during the night grow to a magnitude comparable to $k_2 N_m N_2$. By these times however the changes in N_3 are rather slow and even considering the addition of the terms in the denumerator the assumption appears sound. Thus we get

$$N_3^\tau = a_{31} N_1^\tau + (N_3^t - a_{31} N_1^t) \qquad (19)$$

and inserting this in equation (6) we get for the solution of N_1 at the end of the time step an ordinary differential equation of the form

$$\frac{dN_1}{dt} = aN_1^2 + bN_1$$

where $a = -2k_1 N_m - a_{31} k_3$,

$b = -k_2 N_m N_2 - k_3 N_3^t + a_{31} k_3 N_1^t$.

Equation (19) gives then also N_3 at the end of the time step.

Region III

In the daytime region where $k_2 N_m N_2 + k_3 N_3 > 0.8 \cdot 10^{-2} N_3$ is sensible constant during one time step. By analogous reasons as in region I for N_3 we may say that

$$N_1^t = N_1(E) = (-b - \sqrt{b^2 - 4ac})/2a,$$

where $a = -2k_1 N_m$,

$b = -k_2 N_m N_2 - k_3 N_3^t$,

$c = 2J_2 N_2 + J_3 N_3^t$.

$N_1 = N_1(E)$ is the stationary solution to (6). The new value for N_3 at the end of the time step is obtained by solving the differential equation arrived at by inserting $N_1 = N_1(E)$ in equation (8). The criterium $0.8 \cdot 10^{-2}$ was chosen because by this choice the 20–100 km region is divided into two layers, one where $N_1 > N_3$ and the other where $N_1 < N_3$ at noon.

Region IV

There are levels where during daytime neither the conditions for region I nor those for region III are satisfied. A solution for N_3 at the end of a time step is obtained by inserting $N_1 = N_1^t$ (its value at the beginning of the time step) in equation (8) and solving the obtained ordinary differential equation for N_3.

A similar procedure is used to obtain new N_1 values, now by fixing $N_3 = N_3^t$, inserting in equation (6) and solving the differential equation obtained for N_1.

This region is the least satisfactory from a computational point of view, but it is not expected to introduce systematic errors because this region is a narrow one and because of the physical tendency toward selfcorrection.

Region V

There may be levels where the conditions for both region I and region III are satisfied. To save computer time this new region is introduced. As seen from the considerations made for region I and III $dN_1/dt = dN_3/dt = 0$ and thus a solution may be obtained from the simultaneous evaluation of equations (6) and (8) giving:

$$N_1 = \frac{-b - \sqrt{b^2 - 4ac}}{2a} \quad \text{and} \quad N_3 = \frac{k_2 N_m N_2 N_1}{J_3 + k_3 N_1},$$

where $a = -k_2 k_3 N_m$, $b = J_2 k_3$, $c = J_2 J_3$. Again, to save computer time the term $k_1 N_m N_1^2$ has here been deleted because of its very small size compared to the other terms entering into the exact solution. It should be pointed out that this is the only time in the treatment of the time-dependent model that any reaction is dropped from the equations.

Convergence of solutions

The question of convergence of this model is difficult to evaluate in an analytical fashion. For this reason, a convergence check was introduced into the model. This check consists of storing 62 values of ozone taken from different levels at three selected times and comparing them with the values that occurred twenty-four hours previously. If the concentration changes by less than one per cent of its previous value (twenty-four hours before) the solution at the point is considered to have converged. The three times selected for these comparisons are solar noon, sunset at the earth's surface and sunrise at the earth's surface. After each twenty-four hour period (about ten minutes on the Besk computer) a print-out is provided listing the day number and the total number of points that have not fulfilled the convergence criteria. It was found that in general the number of such points decreases rapidly at first, and more slowly as time progresses. The results of all runs indicate a slow but steady convergence.

Results from the time-dependent model

The numerical results of the time-dependent model will be discussed in terms of five special cases; they are:

1. High latitude summer case (80° Latitude, with polar summer temperature profile).

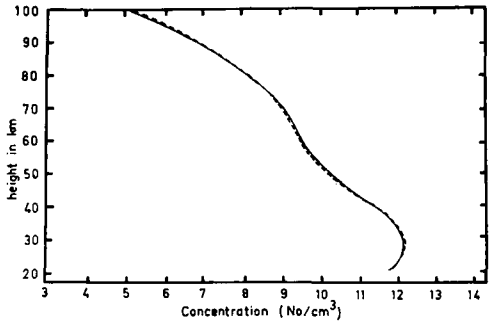

FIG. 5. 80° Latitude, summer, 7 days for convergence, solid line infinite-day guess, dashed line results from time dependent model, concentration powers of 10.

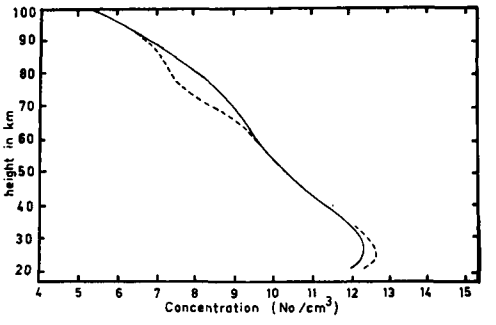

FIG. 7. 0° Latitude, 23 days for convergence, solid line infinite-day guess, dashed line results from time dependent model, concentration in powers of 10.

2. Mid-latitude summer case (45° Latitude, with mid-latitude summer temperature profile).
3. Tropical case (0° Latitude, with tropical atmosphere temperature profile).
4. Mid-latitude winter case (45° Latitude, with mid-latitude winter temperature profile).
5. High latitude winter case (67° Latitude, with polar winter temperature profile).

Latitudinal variations of ozone

Figs. 5, 6, 7, 8 and 9 present the ozone distribution at selected times of day at these latitudes and seasons. The initial guess of the ozone distribution obtained from the infinite-day model is also shown. The number of days taken for the convergence criterion to be met is given below the figures.

From these figures it is evident that certain changes from the infinite-day guess must be explained. The following questions are asked:

1. Why does the time-dependent model give smaller ozone concentrations in the upper levels and larger concentrations in the lower levels than does the infinite-day guess?

2. Why is the above departure nearly absent in the high latitude summer case and appears to become larger as one approaches the high latitude winter case?

These questions are not separable but do result from the same physical processes. That is, if one considers the basic equations (equations 6, 7 and 8) at night, it is seen that dN_1/dt always is less than or equal zero and dN_3/dt is always greater than or equal to zero, while dN_2/dt may be either greater than, equal or less than zero. At the beginning of night at those levels where some atomic oxygen exists, dN_2/dt will be grea-

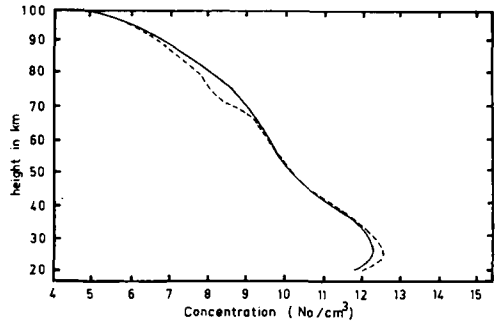

FIG. 6. 45° Latitude, summer, 14 days for convergence, solid line infinite-day guess, dashed line results from time dependent model, concentration in powers of 10.

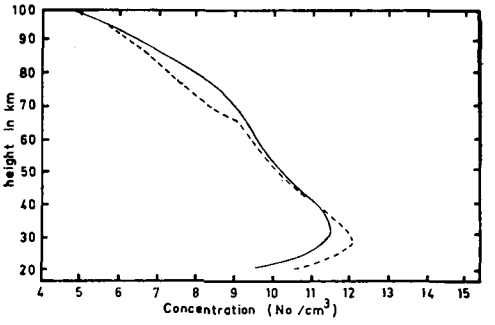

FIG. 8. 45° Latitude, winter, 29 days for convergence, solid line infinite-day guess, dashed line results from time dependent model, concentration in powers of 10.

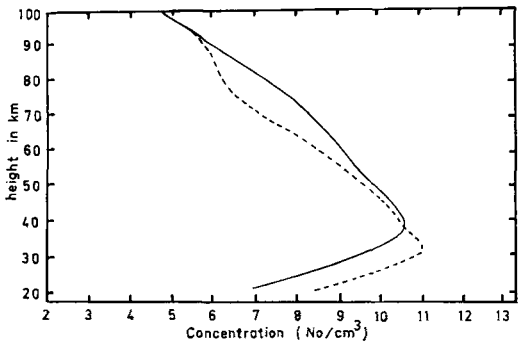

FIG. 9. 67° Latitude, winter, 54 days for convergence, solid line infinite-day guess, dashed line results from time dependent model, concentration in powers of 10.

ter than zero and dN_2/dt will be less than zero as long as

$$N_3 < (k_2 N_m N_2 - k_1 N_m N_1)/2k_3. \quad (20)$$

As seen from equation (8) the maximum possible value of ozone is given by

$$N_3 = k_2 N_m N_2/K_3. \quad (21)$$

This value may be reached only if sufficient atomic oxygen is available. If one compares equations (20) and (21) it is seen that the build up of ozone at night may result first in a decrease of molecular oxygen and then an increase in molecular oxygen. For example, at the 70 km level about 2000 seconds after sunset most of the atomic oxygen being destroyed is being transferred to molecular oxygen rather than to ozone. The process will continue for the remaining period of night or until all the atomic oxygen is destroyed.

With the beginning of daylight, this build-up of ozone is eliminated and the excess concentration is returned to atomic oxygen almost immediately. However, that portion of the atomic oxygen that was transferred to molecular oxygen during the night cannot be completely replaced during the day. There will therefore be a decrease in the amount of atomic oxygen at these leves, from its infinite-day value, until a point is reached when the atomic oxygen concentration is restored to its original value during the day. The result of this decrease in atomic oxygen as seen from equation (8) will be a corresponding decrease in the ozone concentration at these levels.

This process will be of major importance at upper levels and will not occur at lower levels due to the atomic oxygen being so small that equation (20) is always satisfied during night. At the upper levels where the atomic oxygen is large this process will be dependent on the length of night and therefore a function of the latitude and time of year.

The effect of this reduction of the ozone concentration in the upper levels is to reduce the optical path due to ozone and thereby allow the radiation to penetrate to lower levels. Such an increase will produce more atomic oxygen at lower levels and, as seen from equation (8), yield a greater production of ozone. The amount of this build-up of ozone between 20 to 30 km would be dependent on the amount of the reduction in the optical path above. It is therefore seen that this build-up will be a function of the length of night and the intensity of mid-day radiation and thus will be latitude dependent. At very high latitudes the length of night is long in the winter, but the ozone build-up is not as large as may be anticipated due to the low intensity of the radiation during day.

No night occurs in the high latitude summer case and therefore it shows little of the departures discussed above. The infinite day guess based on an average radiation (J_2) is also seen to be a good approximation to the time-dependent solution.

The end result of the above effect is to build and lower the ozone maximum at high to mid-latitudes with very little effect in the equatorial region where the length of night varies little over a year. Fig. 10 shows height of the ozone maximum as a function of latitude as obtained from the infinite-day model, time-dependent model, and that actually observed.

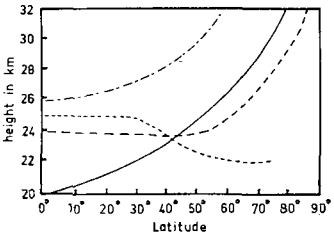

FIG. 10. Height of ozone maximum concentration for: Infinite-day model noon zenith angle (———), Infinite-day model based on average daily radiation (—·—·—), Time-dependent model results (— — —), and actual observed height of maximum ozone layer as given by DÜTSCH 1964 (– – – – –).

The result indicates that it is of vital importance to consider this effect if one is using the difference between the observed ozone distribution and the photochemical distribution as a measure of the circulation or mass transport in the upper levels of the atmosphere. It is obvious that the circulation required to explain the differences between the time-dependent photochemical model and the observed is much less than that required to explain the differences between the infinite-day photochemical model and the observed distribution.

The longitudinal variations of ozone

The longitudinal or daily variation of the ozone concentration for the cases considered is shown in Figs. 11–15. The isolines represent lines of the ratio of the ozone concentration at any given time to its noon value, i.e. $x = N_3^t/N_3^{1200}$.

The most striking features are the build-up of ozone during the night and the resulting excess depletion ($x < 1$) of ozone at sunrise. This is due to the rapid time for dissociation compared to the much slower three-body collisional process. Such an effect, when integrated over a year, may also yield a phase lag in the seasonal build-up and destruction of ozone, that is the minimum total ozone concentration may occur during the late winter rather than at the winter solstice.

It is seen that the magnitude of the x-ratio maximum is in general larger the longer the night. This however does not mean that the magnitude of ozone at the end of night is appreciably different. The maximum possible concentration of ozone at night in the 70 to 80 km layer is a function of the pressure and temperature distribution which determines the concentration of molecular oxygen and the third body. The temperature distribution in part also determines the value of the rate coefficients k_2 and k_3. The x-ratio, however, is inversely dependent upon the concentration at noon; therefore, the maximum value of x becomes larger the smaller the noon value. Since this is the region of the reduction of ozone due to the previously discussed mechanism, it is obvious that the ratio must therefore be latitudinally dependent for given meteorological conditions. The ratio is higher at latitudes where the duration of night is long and lower at latitudes where the length of night is short. The effect of meteorological conditions, that is temperature and pressure distribution, may override this effect as seen in Fig. 15.

In addition to the isolines of the x ratio, Fig. 15 also has two lines on either side of solar noon marked J_2 and J_3. Along these lines the radiation represented by these dissociation rate coefficients becomes essentially zero, i.e. less or equal 10^{-38} sec^{-1}. This graphically shows the effect of the difference in the mean absorption as represented by their respective spectral ranges. The J_3 dissociation coefficient is the first to come into existence at sunrise and the rate of destruction of ozone is very large until the J_2 dissociation coefficient becomes large enough to increase the atomic oxygen by dissociation of molecular oxygen and thereby increasing the ozone concentration.

The annual variations of ozone

The preceding analysis indicated that an integration over a year at a given latitude was desirable in order to determine if a seasonal phase lag did exist in the photochemical distribution as obtained by the time-dependent model. The simplifying assumptions made and the method of approach to this yearly integration is as follows:

1) The solar latitude was assumed to vary as a sine wave between the latitudes of 22½° N and 22½° S, with a period of 364 days. Its most northerly position was at the summer solstice and most southerly position during the winter solstice for the northern hemisphere.
2) The solar latitude was taken as constant during the number of days required for the sun to change its noon position by 5° of latitude. The solar latitude used during such a period was represented by its mid-point, for example, a solar latitude of 15° N was used for the time during which the sun at solar noon was between 17½° N to 12½° N.
3) The yearly integration was conducted for mid-latitude (45° N) using the ICAO standard atmosphere distribution at all times of year. This procedure in effect removes all of the seasonal temperature dependence. A future experiment is planned in which the seasonal temperature dependence will be considered.

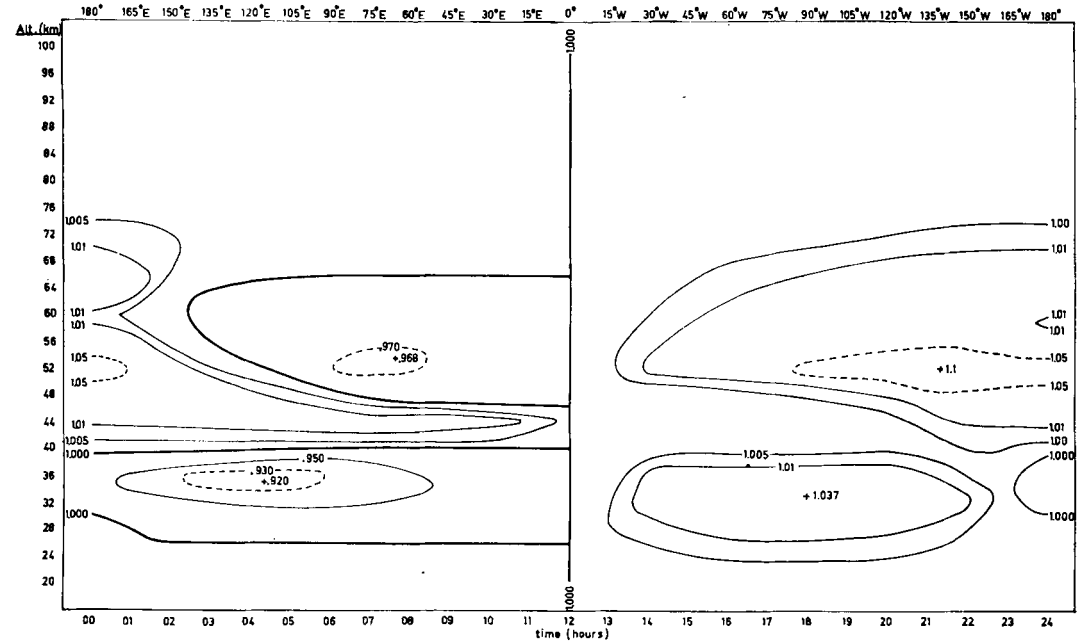

FIG. 11. 80° Latitude, summer, isolines of x, where $x = N_3^t/N_3^{1200}$.

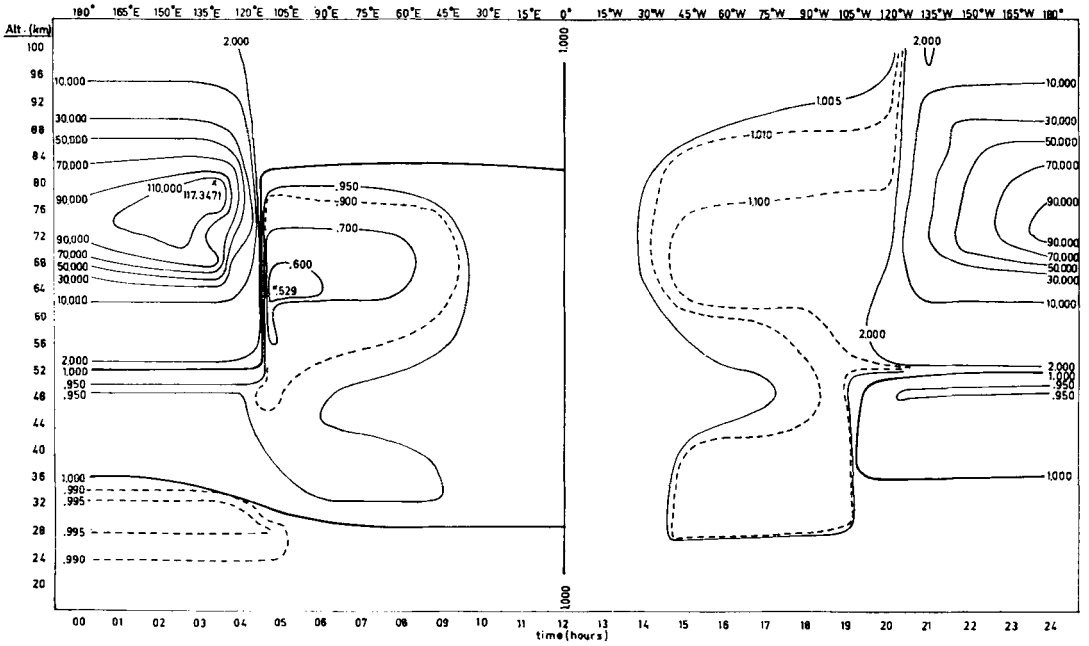

FIG. 12. 45° Latitude, summer, isolines of x, where $x = N_3^t/N_3^{1200}$.

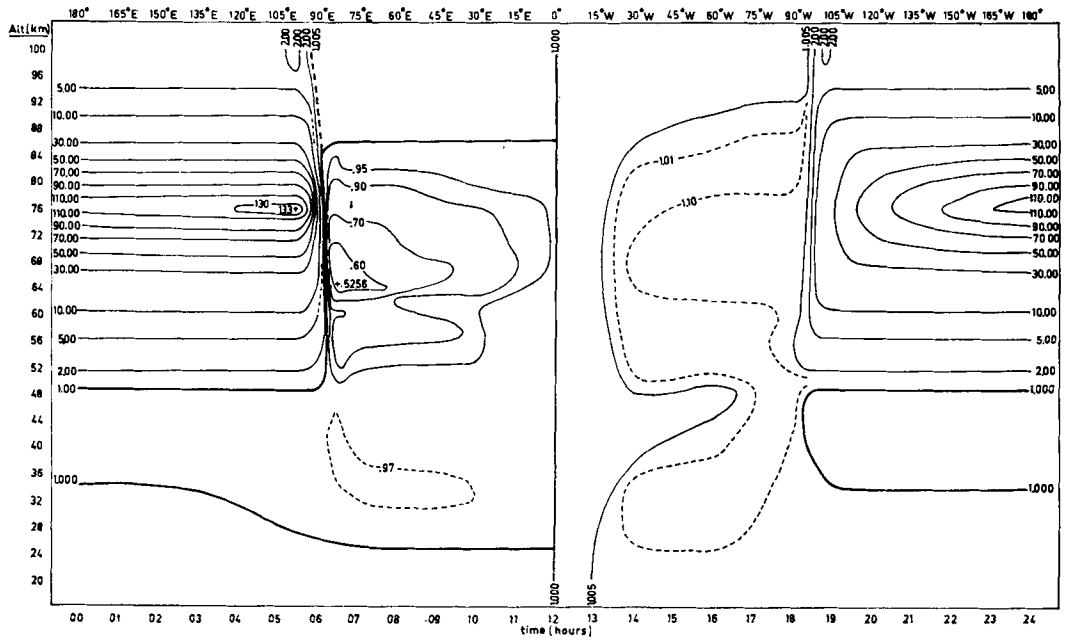

FIG. 13. 0° Latitude, isolines of x, where $x = N_3^t/N_3^{1200}$.

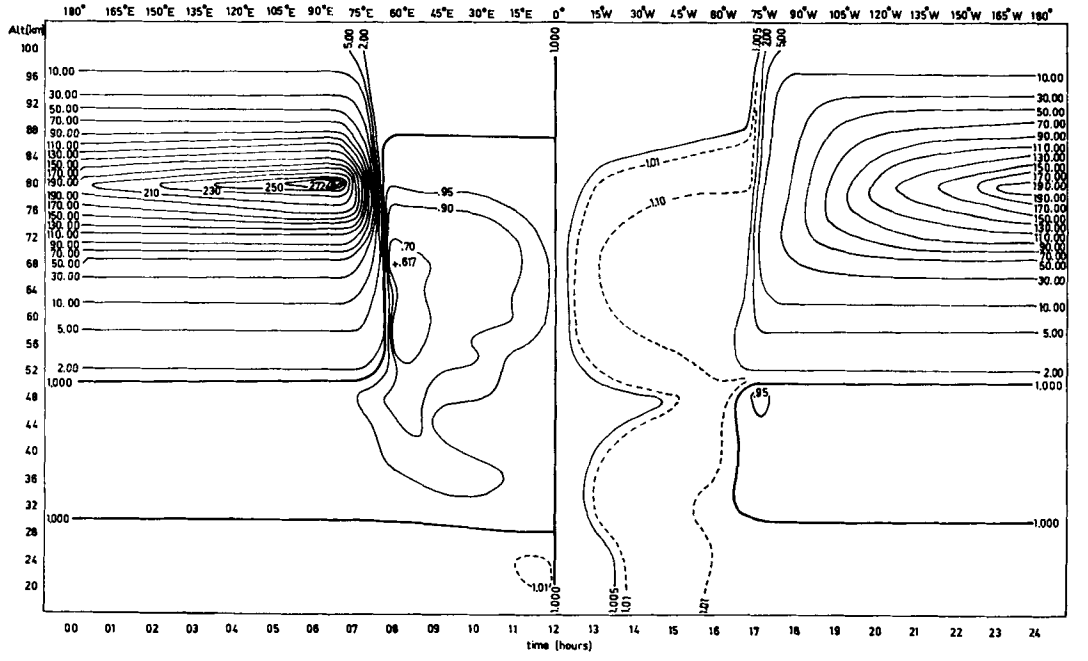

FIG. 14. 45° Latitude, winter, isolines of x, where $x = N_3^t/N_3^{1200}$.

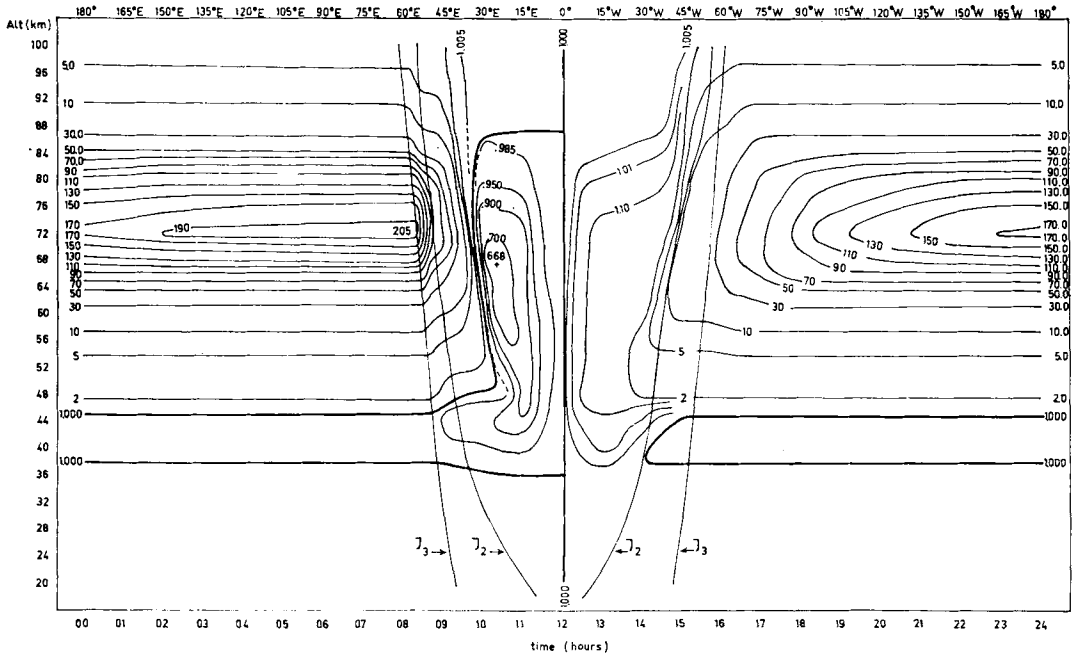

FIG. 15. 67° Latitude, winter, isolines of x, where $x = N_3^t / N_3^{1200}$.

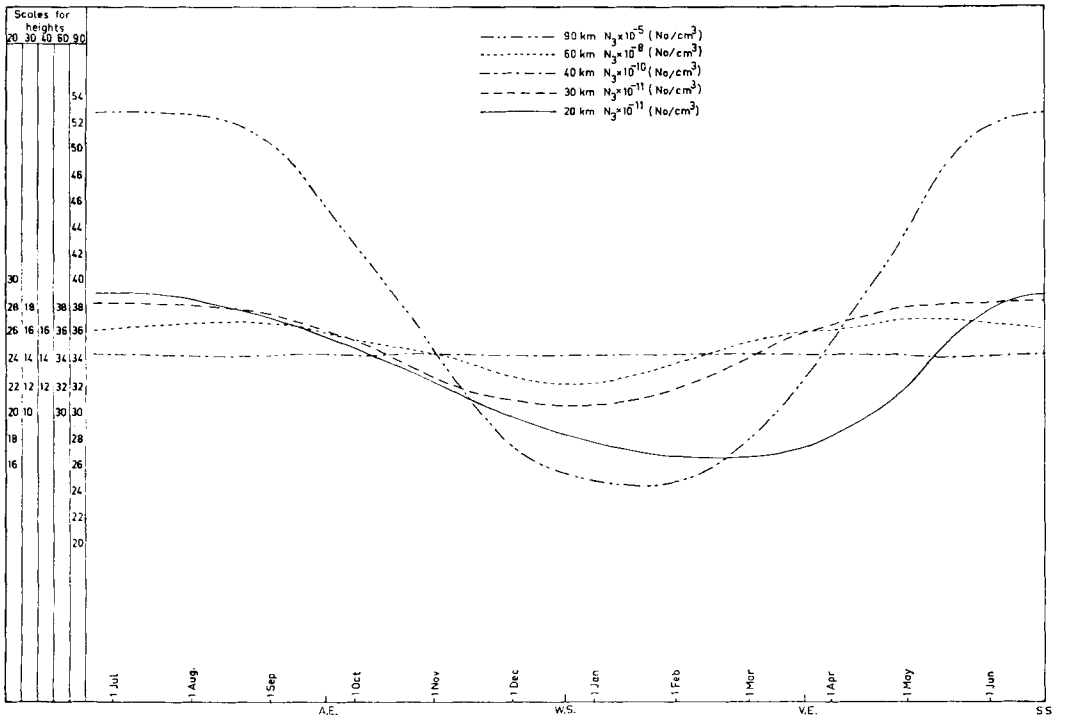

FIG. 16. Yearly variation of ozone concentration at five selected levels.

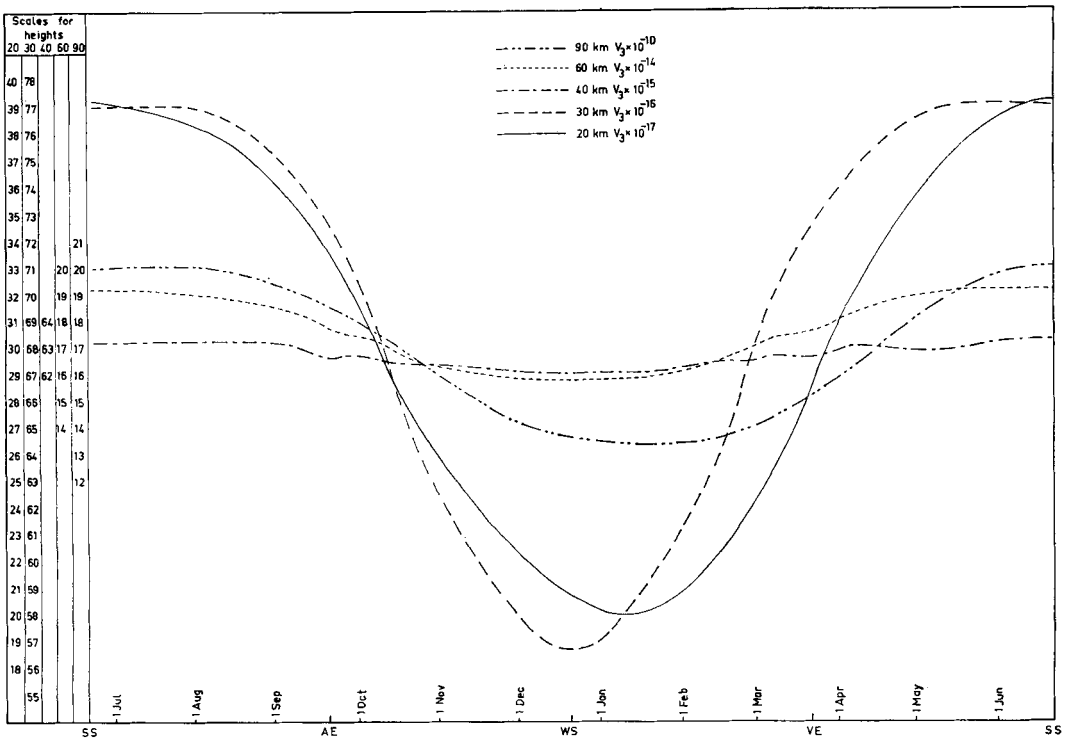

FIG. 17. Yearly variation of volume of ozone above a cm² area at five selected levels.

From the preceding discussions it is evident that the time for adjustment to changing radiation is different for radiation increasing than for radiation decreasing. During the time of year from the summer solstice through the autumnal equinox to the winter solstice the incoming radiation is being progressively reduced. The adjustment to this reduction in the radiation must be brought about by the relatively slow collisional processes. However, during the period between the winter solstice through the vernal equinox to the summer solstice the radiation is progressively increasing. The adjustment to increasing radiation is by molecular dissociation and is relatively fast in comparison to the collisional adjustment process. This may therefore lead to the development of a lag such that the minimum ozone concentration at a given level may occur not at the winter solstice but at a later time.

Fig. 16 gives the concentration of ozone for five selected levels as a function of time-of-year. At 90 km and at 20 km the expected seasonal lag exists. The minimum concentrations for these levels occur 27 days and 56 days respectively after the winter solstice. The phase shift is approximately zero for the mid-heights from 30 to 60 km. This result is in agreement with the height dependence of the time constants as shown by HESSTVEDT (1963).

Another interesting feature is that the relative amplitude of the concentrations decreases toward the 40 km level. At 40 km the concentrations appear to be almost independent of changing zenith angle. LONDON (1962) also has found that the mid height range showed a minimum sensitivity to zenith angle influences.

It is also of interest to determine how these phase shifts affect the total ozone concentration. Fig. 17 gives the number of ozone molecules above a square centimeter area at selected levels.

The minimum total ozone above 90 km is found to occur 32 days after the winter solstice. No significant lag is found in the mid-height range and the lag does not appear again until the lower levels are reached. At 20 km the integrated effect of all levels and all lags is

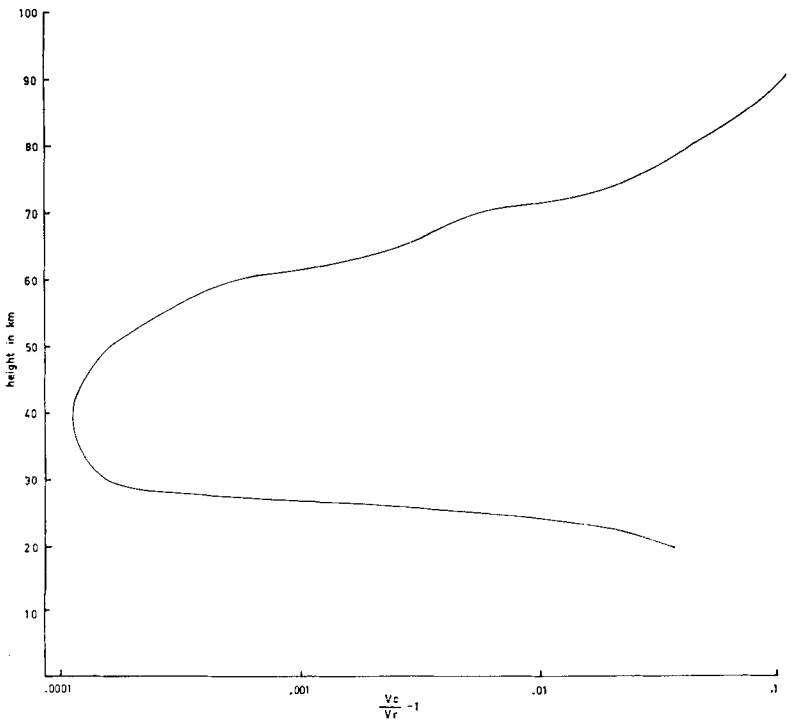

FIG. 18. The height variation of the ratio of the volume of ozone above 20 km in early summer to that in late summer where the solar latitude is 15° in both cases.

shown with the result that the minimum total ozone is found to occur 22 days after the winter solstice.

In view of the two physical processes working at different times of the year to bring ozone into agreement with the existing radiation, it is of interest to compare the vertically integrated volume just before and just after the summer solstice period. This comparison is made during the time when the solar latitude is 15° N. Fig. 18 gives such a comparison where V_R represents the vertically integrated volume in early summer and V_c represents the volume in late summer. The effect of the variation of adjustment times is strikingly shown. HESSTVEDT (1963) found that the adjustment in a pure oxygen atmosphere was determined by two characteristic times. The initial adjustment was controlled by an extremely fast characteristic time (τ_1) of less than a minute at all levels. The final adjustment however was controlled by a much slower characteristic time (τ_2). τ_2 varied from months at the low levels to minutes at about 50 km and then increased again to months at about 100 km. The regions of solutions used in the time-dependent model are in agreement with this analysis of the characteristic times and their variation in height and season in a pure oxygen atmosphere. The assumptions of an immediate adjustment of ozone in region I and of atomic oxygen in region III are expressed by Hesstvedt's τ_1 adjustment time. The constancy of atomic oxygen in region I and of ozone in region III are expressed by τ_2. Region V corresponds to that part where both τ_1 and τ_2 are much shorter than a time step. Region IV may be inferred from Hesstvedt's results by comparing the changes of the characteristic times with season. Region II is solely due to the existence of night in the time dependent model.

Comments

It should be stressed that the results given in this paper are not considered quantitatively exact. The rate coefficients chosen were believed by the writers to be the best available based upon considerations made in the first portion

of this paper. The magnitude of the time and space variations of the ozone concentrations and their interactions with other levels is dependent upon the accuracy of the rate coefficients, in particular the dissociations rate coefficients which are themselves dependent upon the accuracy of the absorption coefficients. The absorptivity changes rapidly with wavelength and the smoothed absorption assumed for the spectrum in this study tends to underestimate the absorption at some levels and overestimate the absorption at other levels. The errors due to such an approximation may therefore affect the magnitude or level of these variations. However, the existence of the phase lags and their interactions depend upon the difference in adjustment time by dissociation and by collisional processes and are therefore believed to be a physical reality and may be of considerable importance in the seasonal variation of the photochemical ozone concentration.

The numerical method used to compute the rate coefficients was the same in both the infinite day and the time-dependent model. Therefore, the differences of the results between these two models are independent of the computational procedure used to obtain the rate coefficients.

The present programs have been made general and may accept any rate coefficients, temperature and pressure profiles, geographic locations and height and time steps. They will however be modified to accept continuous rather than stepwise changes in the meteorological parameters and in the sun's zenith angle. Thereafter they will be used for yearly integrations of the ozone amounts at 0°, 30°, 45°, and 60° latitude. The program will also be used for study of the effects of variations of meteorological parameters and of the sun's radiational input.

REFERENCES

Chapman, S., 1930, A theory of upper atmospheric ozone. *Mem. Roy. Soc.*, **3**, pp. 103–125.

Dütsch, H. U., and Carlton, L. M., 1964, Uniform evaluation of Umkehr observations from the World Ozone Network. Part II, Summary Supplement, The vertical distribution of ozone. National Center for Atmospheric Research, Boulder, Colorado.

Hesstvedt, E., 1963, On the determination of characteristic times in a pure oxygen atmosphere. *Tellus*, **15**, 1, pp. 82–88.

Hesstvedt, E., 1965, Some characteristics of the oxygen-hydrogen atmosphere. *Geofysiske Publikasjoner*, **26**, No. 1.

Johnson, F., 1954, The solar constant. *J. Meteor.*, **11**, pp. 431–439.

Leovy, C., 1963, Mesospheric heating and simple models of thermally driven circulation. Doctoral Thesis, M.I.T.

London, J., 1962, Mesosphere dynamics. Final report, New York University. Contract No. AF19 (604)-5492.

Nicolet, M., 1960, Properties and constitution. *Physics of the Upper Atmosphere*, Academic Press, **2**, pp. 17–69.

Ohring, G., 1958, The radiation budget of the stratosphere. *J. Meteor.*, **15**, pp. 440–450.

Plass, G., 1956, The influence of the 9.6 μ ozone band on the atmosphere infra-red cooling rate. *Roy. Met. Soc.*, **82**, pp. 3043.

Handbook of Geophysics, 1960. The Macmillan Company, New York, Chapter 8, p. 5.

ФОТОХИМИЧЕСКАЯ МОДЕЛЬ ДЛЯ ПРОСТРАНСТВЕННО-ВРЕМЕННЫХ ИЗМЕНЕНИЙ ОЗОНА В СЛОЕ ОТ 20 ДО 100 КМ

Исследуются различные стационарные фотохимические модели (модели «бесконечного дня»). Выяснено влияние на свойства этих моделей пренебрежения некоторыми фотохимическими реакциями. В рассмотренной стационарной модели было пренебрежено девятью реакциями.

Нестационарная модель была развита с помощью интегрирования по времени за период в 1 день. Эта модель дала распределение атомного, молекулярного кислорода и озона как функцию высоты, широты, времени дня и метеорологических условий в данное время года.

Результаты, полученные с помощью обеих этих моделей были сравнены между собой и с данными наблюдений. Найдено, что нестационарная модель во многих случаях дает более хорошее совпадение с данными наблюдений, чем стационарная.

Сезонный сдвих фазы был получен интегрированием по времени за 1 год. Этот сдвиг фаз представлен как функция времени года и высоты при заданной широте.